DESIGN AND FORCE RESPONSE FOR A MESH-TYPE ROTARY PIEZOELECTRIC MOTOR

Chong LI,[1], Jichun XING[2]

A mesh-type rotary piezoelectric motor is designed in which piezoelectric drive principle is combined with harmonic drive and movable tooth drive principles, and sliding friction between rotor and stator is changed into rolling meshing. And the principle of the proposed motor is illustrated. Using planetary transmission for reference, the dynamic models of movable tooth drive system of the motor are established. Moreover, the forced response equations of the system are deduced. The laws of time responses and frequency responses of the motor are revealed. Results show that torsional vibrations displacements of central elements (wave generator, rigid cog and rotor) are larger than translational vibration when the system resonates. These results provide theoretical basis for improving the performance and avoiding the resonance of the mesh-type rotary piezoelectric motor.

Keywords: piezoelectric motor, force response, movable tooth drive, dynamic model.

1. Introduction

Over recent years, with higher efficiency mechanical transmission required, piezoelectric driving has become a top research field [1-3]. Piezoelectric motors have been utilized in the field such as precision actuating, accurate positioning, energy harvesting and vibration control [4-7].

Rudy proposed a traveling wave piezoelectric motor with diameter of 3 mm [8]. Ho designed a piezoelectric screw- driven motor operating in shear vibration modes, and the translational velocity of the motor was 2.137 mm/s when applying 16 V peak voltage without mechanical load [9]. Besides, a traveling wave rotary ultrasonic motor was developed by Renteria [10]. In conventional piezoelectric motors, the driving mechanism mainly is via friction between stator and rotor, but the contact friction results in shortened lifetimes and higher temperature.

Hence, a non-contact piezoelectric motor was proposed [11,12]. The non-contact motors eliminate the friction between the stator and rotor, and increase the efficiency and lifetime. However, the output torque of it is too small to satisfy the practical need. Therefore, a new piezoelectric motor is necessary.

[1] Jiangsu University of Science and Technology, China, email: lichong@just.edu.cn
[2] Yanshan University, China, email: xingjichun@ysu.edu.cn

As a result, harmonic piezoelectric motor was designed and fabricated, and the output torque of which is at approx 0.75 Nm [13]. Besides, a harmonic piezoelectric motor which is equipped with fixed piezoelectric actuator and displacement amplifier was developed [14]. Nevertheless, despite the high output torque and operating life now achieved as a result of such an effort, the harmonic gear is facing machining difficulty and expensive material, etc.

In view of that, the authors proposed a mesh-type rotary piezoelectric motor. And the motor integrates piezoelectric drive, the movable tooth drive and the harmonic drive principles in order to obtain a large output torque as well as a speed reduction. Besides, the piezoelectric motor can also fill the gaps in low life expectancy and efficiency. In addition, the rigid cog and other elements of the motor are easy to machine with the best processing charges.

As a transmission device, vibration characteristics have a great influence on the performance of the motor. However, few research on force response of mesh-type rotary piezoelectric motor has been investigated up to now. So the objective of this research is to reveal the vibration characteristics of the mesh-type rotary piezoelectric motor.

2. Design for the motor

The mesh-type rotary piezoelectric motor shown in Fig. 1 consists of driving system and transmission system. The working principle of the motor is presented in Fig. 2. In Figs. 1 and 2, the driving system includes (1) piezoelectric actuator, (2) z-shaped rod, (3) swaying rod and (8) adjusting spring. The transmission system contains (4) movable tooth, (5) rigid cog, (6) rotor and (7) wave generator. When the motor works, two bar-type piezoelectric actuator that are placed at 90° to each other are utilized to drive the displacement amplification mechanism (composed of (2) z-shaped rod and (3) swaying rod) to generate a continuous harmonic wave at the edge of (7) wave generator. The periodic motion of wave generator drives the movable teeth to mesh with (5) rigid cog causing (4) rotor fit to rotation. Hence, a lower speed and a larger output torque can be obtained.

3. Dynamic models and equations

Dynamic model of drive system of mesh-type rotary piezoelectric motor is shown in Fig. 3. The Figs. 3(a) and (b) are the relative displacement between movable teeth and central elements (rotor, rigid cog and wave generator) and forces of movable tooth system, respectively. In Fig. 2, the coordinate system *OXY* is attached to the foundation, *oxy* to rotor 4, and $o_i x_i y_i$ to the *i*-th movable tooth. Subscript *s*, *c*, *r*, *p* represent, respectively, wave generator, rigid cog, rotor and movable tooth. Besides, x_j, y_j, u_j represent *x*, *y* direction and circumferential

direction linear displacement ($j = s, c, r, p_1 \ldots, p_z$).

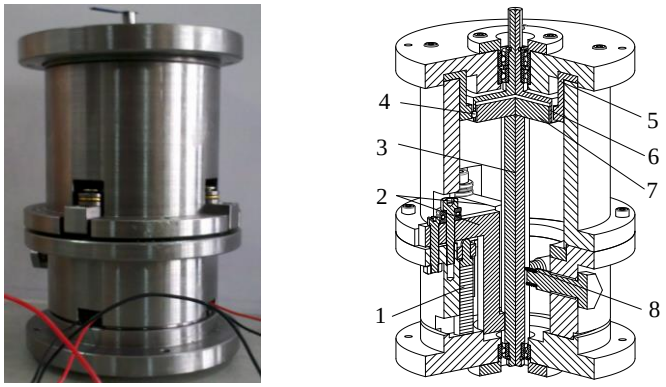

(a) Prototype (b) Solid model

Fig. 1. Mesh-type rotary piezoelectric motor

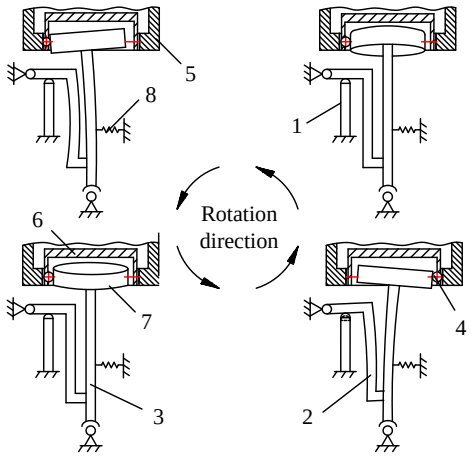

Fig. 2. Working principle of the mesh-type piezoelectric motor

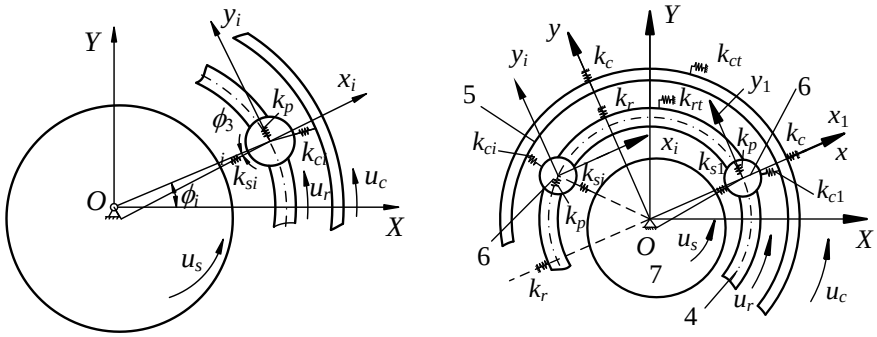

(a) Relative displacement (b) Forces of movable tooth system

Fig. 3. Dynamic model of drive system of the motor

From Fig. 3(a), the projection of relative displacement from central elements to movable teeth along meshing line can be written as [15]

$$\begin{cases} \delta_{si} = \left(x_s - x_{pi}\right)\cos\phi_{1i} + \left(y_s - y_{pi}\right)\sin\phi_{1i} + u_s \sin\phi_{3i} \\ \delta_{ci} = \left(x_c - x_{pi}\right)\cos\theta_i + \left(y_c - y_{pi}\right)\sin\theta_i - u_c \sin\phi_{\theta i} \\ \delta_{ri} = \left(x_{pi} - x_r\right)\sin\phi_i + (y_r - y_{pi})\cos\phi_i - u_r \end{cases} \tag{1}$$

where $\phi_{1i}= \phi_i+\phi_{3i}$, $\phi_{\theta i}=\phi_i-\theta_i$. θ_i is angular displacement of elements, ϕ_i is the angle between line oo_i and coordinate axis x direction, oo_n is the line from center of the n-th movable tooth to rotor center, and ϕ_{3i} is the angle between line oo_{3i} and coordinate axis x direction, oo_{3i} is the line from center of the n-th movable tooth to vibrator center.

From Fig. 3(b), the dynamic equations of drive system for the mesh-type piezoelectric motor can be expressed by

$$\begin{cases} m_s\ddot{x}_s + \sum_{i=1}^{Z} k_s\delta_{si}\cos\phi_{1i} + k_{sz}x_s = 0 \\ m_s\ddot{y}_s + \sum_{i=1}^{Z} k_s\delta_{si}\sin\phi_{1i} + k_{sz}y_s = 0 \\ \left(I_s / r_s^2\right)\ddot{u}_s - \sum_{i=1}^{Z} k_s\delta_{si}\sin\phi_{3i} + k_{st}u_s = T_s / r_s \\ m_c\ddot{x}_c + \sum_{i=1}^{Z} k_c\delta_{ci}\cos\theta_i + k_{cz}x_c = 0 \\ m_c\ddot{y}_c + \sum_{i=1}^{Z} k_c\delta_{ci}\sin\theta_i + k_{cz}y_c = 0 \\ \left(I_c / r_c^2\right)\ddot{u}_c - \sum_{i=1}^{Z} k_c\delta_{ci}\sin\phi_{\theta i} + k_{ct}u_c = 0 \\ m_r\ddot{x}_r - \sum_{i=1}^{Z} k_r\delta_{ri}\sin\phi_i + k_{rz}x_r = 0 \\ m_r\ddot{y}_r + \sum_{i=1}^{Z} k_r\delta_{ri}\cos\phi_i + k_{rz}y_r = 0 \\ \left(I_r / r_r^2\right)\ddot{u}_r - \sum_{i=1}^{Z} k_r\delta_{ri} + k_{rt}u_r = 0 \\ m_p\ddot{x}_{pi} - k_c\delta_{ci}\cos\theta_i + k_r\delta_{ri}\sin\phi_i - k_s\delta_{si}\cos\phi_{1i} = 0 \\ m_p\ddot{y}_{pi} - k_c\delta_{ci}\sin\theta_i - k_r\delta_{ri}\cos\phi_i - k_s\delta_{si}\sin\phi_{1i} = 0 \\ \left(I_p / r_p^2\right)\left(\ddot{u}_i + \ddot{u}_j\right) = 0 \end{cases} \tag{2}$$

where m_j, I_j are mass and relative mass of each element, k_j, k_{jz} and k_{jt} represent the mesh stiffness, radial and tangent supporting stiffness between the movable teeth and central elements, r_i is theoretical radius of elements, and T_s is output torque of

wave generator.

Eq. (2) can be written in matrix form as

$$\boldsymbol{M}\ddot{\boldsymbol{q}}+\boldsymbol{C}\dot{\boldsymbol{q}}+\boldsymbol{K}\boldsymbol{q}=\boldsymbol{F}_z \tag{3}$$

where $\boldsymbol{q}$ is the generalized coordinate vector of transmission system;, $\boldsymbol{M}$ is the mass matrix of the system; $\boldsymbol{K}$ and $\boldsymbol{C}$ is the stiffness and damping matrix, respectively; $\boldsymbol{F_z}$ is incentive force, $\boldsymbol{F_z}$ =[0 0 $T_s$sin($w_s t$)/r_s 0 0 0 … 0 0 0]$^{\mathrm{T}}$.

Assuming the modal shape matrix is $\boldsymbol{A_p}$, then the primary mass matrix can be expressed as $\boldsymbol{M}_p=\boldsymbol{A}_p^T\boldsymbol{M}_z\boldsymbol{A}_p$, regular modal matrix as $\boldsymbol{A_N}$, here, $A_N^{(j)}=A_p^{(j)}/\sqrt{M_{p,i}}$. From regular matrix, the regular mass matrix, regular stiffness matrix, regular damping matrix and regular incentive force matrix can be calculated in the forms as $\boldsymbol{M}_N=\boldsymbol{A}_N^T\boldsymbol{M}\boldsymbol{A}_N$, $\boldsymbol{K}_N=\boldsymbol{A}_N^T\boldsymbol{K}\boldsymbol{A}_N$, $\boldsymbol{C}_N=\boldsymbol{A}_N^T\boldsymbol{C}\boldsymbol{A}_N$, $\boldsymbol{F}_N=\boldsymbol{A}_N^T\boldsymbol{F}$.

Hence, the regular differential equation of movable tooth system can be written as

$$\boldsymbol{M}_N\ddot{\boldsymbol{q}}_N+\boldsymbol{C}_N\dot{\boldsymbol{q}}_N+\boldsymbol{K}_N\boldsymbol{q}_N=\boldsymbol{F}_N \tag{4}$$

According to Eq. (4), the *i*-th order regular differential equation can be expressed by

$$\ddot{q}_{Ni}+2\gamma_i\omega_i\dot{q}_{Ni}+\omega_i^2 q_{Ni}=F_{Ni} \tag{5}$$

where γ_i is relative damping coefficient, and $\gamma_i=C_{Ni}/(2\omega_i)$.

From Duhamel's integral, letting initial displacement and vector are zero, the regular displacement response can be written as

$$\begin{aligned} q_{Ni}=&\frac{A_{Ni}^{(3)}T_s}{r_s\omega_{ri}\left[\left(\omega_{ri}^2-\omega_s^2\right)^2+\gamma_i^2\omega_i^2\left(\gamma_i^2\omega_i^2+2\omega_{ri}^2+2\omega_s^2\right)\right]}\cdot\\ &\left\{e^{-\gamma_i\omega_i t}\omega_s\left[\left(\gamma_i^2\omega_i^2+\omega_{ri}^2+\omega_s^2\right)\sin\omega_{ri}t+2\gamma_i\omega_i\omega_{ri}\cos\omega_{ri}t\right]\right.\\ &\left.+\omega_{ri}\left[\left(\gamma_i^2\omega_i\omega_{ri}+\omega_{ri}^2-\omega_s^2\right)\sin\omega_s t-2\gamma_i\omega_i\omega_{ri}\omega_s\cos\omega_s t\right]\right\} \end{aligned} \tag{6}$$

In Eq. (6), displacement response of the system contains transient response and steady response. However, transient response decays with time quickly, steady response exists throughout. Therefore, the steady response of the system can be expressed by

$$\begin{aligned} q_{Ni}&=\frac{A_{Ni}^{(3)}T_s\left[\left(\gamma_i^2\omega_i\omega_{ri}+\omega_{ri}^2-\omega_s^2\right)\sin\omega_s t-2\gamma_i\omega_i\omega_{ri}\omega_s\cos\omega_s t\right]}{r_s\left[\left(\omega_{ri}^2-\omega_s^2\right)^2+\gamma_i^2\omega_i^2\left(\gamma_i^2\omega_i^2+2\omega_{ri}^2+2\omega_s^2\right)\right]}\\ &=\frac{A_{Ni}^{(3)}T_s\sqrt{A^2+B^2}}{r_s}\cos\left(\omega_s t-\alpha\right) \end{aligned} \tag{7}$$

where $\alpha=\arctan\left(-\dfrac{A}{B}\right)$, $A=\dfrac{\gamma_i^2\omega_i\omega_{ri}+\omega_{ri}^2-\omega_s^2}{\left(\omega_{ri}^2-\omega_s^2\right)^2+\gamma_i^2\omega_i^2\left(\gamma_i^2\omega_i^2+2\omega_{ri}^2+2\omega_s^2\right)}$,

$$B = \frac{2\gamma_i \omega_i \omega_{ri} \omega_s \cos \omega_s t}{\left(\omega_{ri}^2 - \omega_s^2\right)^2 + \gamma_i^2 \omega_i^2 \left(\gamma_i^2 \omega_i^2 + 2\omega_{ri}^2 + 2\omega_s^2\right)}.$$

So displacement response of original coordinate can be written as $\boldsymbol{q} = \boldsymbol{A}_N \boldsymbol{q}_N$. Applying Laplace transform to Eq. (4), the system's transfer function can be obtained. Furthermore, frequency response of movable tooth system can be achieved.

4. Results and discussion

In order to explore the vibration characteristics of movable tooth drive system of the motor, the parameters of Table 1 are employed as numerical example. Here, it should be noted that the damping of each element $c_{\zeta i}$ is defined as a constant value.

Table 1

The system parameters

Symbol	Rotor	Rigid cog	Wave generator	Movable tooth
m_j (kg)	1.31×10^{-2}	5.64×10^{-2}	2.59×10^{-2}	3.30×10^{-5}
I_j (kg)	9.34×10^{-3}	8.41×10^{-2}	1.30×10^{-2}	1.32×10^{-5}
r_j (mm)	15.8	16.6	14.5	1
k_{jz} (N/m)	5×10^{8}	5×10^{8}	5×10^{8}	0
k_{jt} (N/m)	0	1×10^{9}	0	0
k_j (N/m)	1×10^{8}	2×10^{8}	1×10^{8}	0

4.1. Time Response of the System

When the outer exciting force T_s/r_s=6.33N and exciting frequency ω_s=1000rad/s are applied to Eq.(7), the steady time response of movable tooth system can be obtained (see Fig. 4). Here, only two movable teeth are selected as research target. From Fig. 4, it is known that:

(1) As the system is excited by harmonic signal come from piezoelectric actuator, so response curves are sinusoid. Period of each response is the same, but phase varies.

(2) The largest displacement (0.035mm) of the drive system for the motor occurs in u_s direction of wave generator. It is because the exciting force is applied on wave generator.

(3) Displacement of torsional vibration of wave generator is much larger than that of translational vibration. However, the translational displacement of rigid cog is larger than that of torsional vibration. The vibration form of rotor is

similar with wave generator. However, the displacement between torsional and translational vibration is smaller.

(4) When building the dynamic model of movable teeth, only two-dimensional motion is considered, so the torsional vibrations of movable teeth are zero. The *x* and *y* directional vibrations of 1st and 2nd movable teeth are large, but the gap of the phase difference between *x* and *y* directional vibrations of 1st movable tooth is π, and 2nd one is zero.

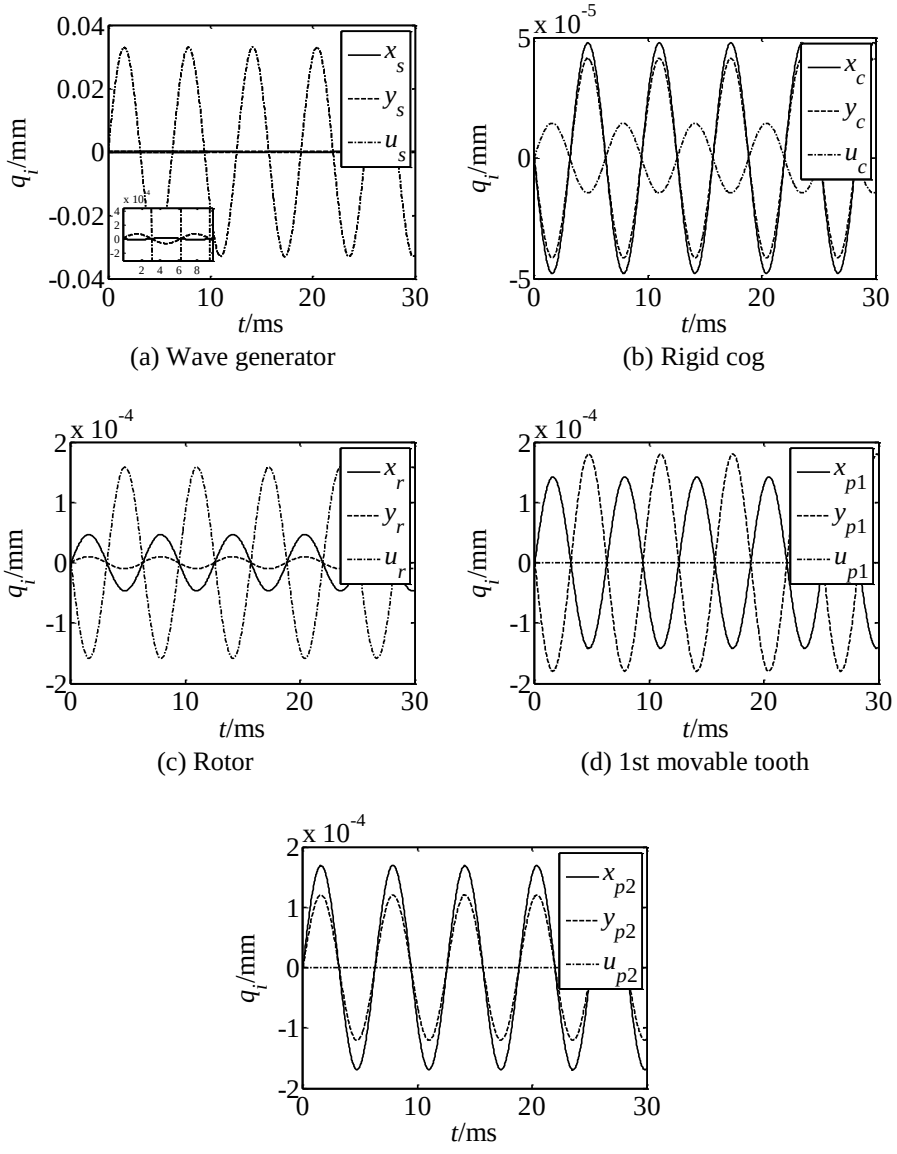

(a) Wave generator (b) Rigid cog

(c) Rotor (d) 1st movable tooth

(e) 2nd movable tooth

Fig. 4. Time response of the drive system under outer incentive

4.2. Frequency Response of the System

The Frequency response of the system is also investigated, and its results are shown in Fig. 5. Here, Frequency range from 0 to 1.5×10^5 rad/s is selected to observe the resonance of drive system for the proposed piezoelectric motor. From Fig. 5, it shows:

(1) When the exciting frequency is close to lowest natural frequency (2093 rad/s), elements of the drive system resonate. Moreover, amplitudes of u_s, u_r, y_{p1} and y_{p2} are largest for corresponding elements. When the exciting frequency is close to 60582 rad/s or 106758 rad/s, elements of movable tooth system resonate as well.

(2) The largest resonance amplitude of the drive system occurs in us direction of wave generator. In addition, for the same order resonance frequency, the resonance amplitudes of u_c and u_r are larger than x_i and y_i. Thus it shows that the displacement of torsional vibration is larger than that of translational vibration.

(3) For movable teeth, the resonance amplitudes of translational vibration are larger than that of central elements (wave generator, rigid cog and rotor).

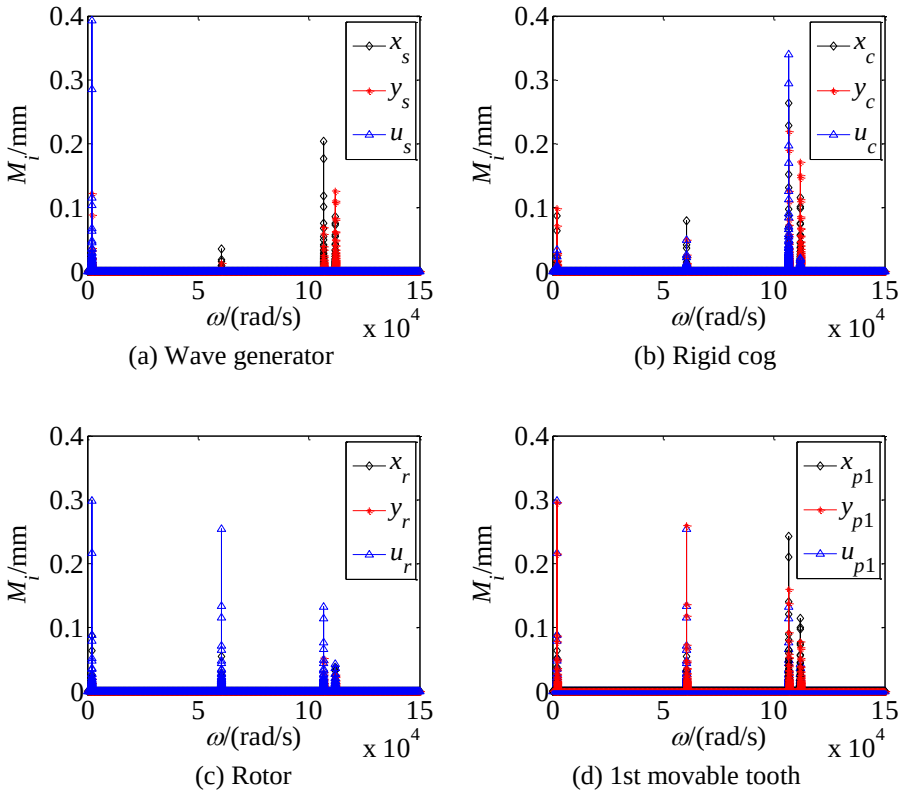

(a) Wave generator (b) Rigid cog

(c) Rotor (d) 1st movable tooth

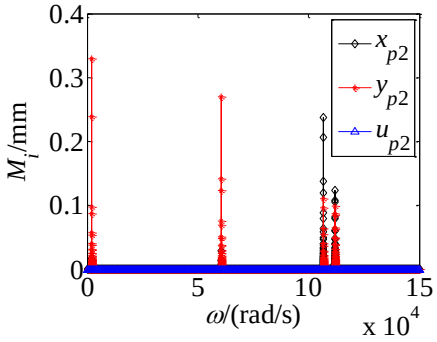

(e) 2nd movable tooth

Fig. 5. Frequency response of the drive system

4.3. Comparison and Analysis of Parameters Influence

Table 2 gives comparison of force vibration of each element, and Table 3 gives changes of resonance amplitude with parameters. They show:

Table 2

Comparison of force vibration for each element

Wave generator		Rigid cog		Rotor		Movable tooth	
M_s	Dir.	M_c	Dir.	M_r	Dir.	M_p	Dir.
2093rad/s	u_s	106758rad/s	u_c	2093rad/s	u_r	2093rad/s	y_{p1}

Here, M_j and Dir. represent vibration frequency for maximum amplitude and its vibration direction.

Table 3

Changes of response amplitude with parameters

Element	r_p (mm)			Δ(%)
	0.5	1	1.5	
Wave generator	0.0351	0.0352	0.0348	1.14
Rigid cog	0.0794	0.0797	0.0788	1.13
Rotor	0.2534	0.2543	0.2513	1.18
Element	a (mm)			Δ(%)
	0.04	0.07	0.1	
Wave generator	0.027	0.0269	0.027	0.0269
Rigid cog	0.0615	0.0614	0.0615	0.0614
Rotor	0.1951	0.1952	0.1951	0.1952

(1) For central elements, the largest amplitudes occur in tangential direction. At 2093 rad/s, most elements except rigid cog behave primary resonance.

(2) As radius of movable tooth rp and offset of wave generator a increase,

the resonance displacement changes. However, the changing rate of rp is larger than a for each element.

(3) The displacement resonance of rotor is largest whether the parameters change or not.

Fig. 6 gives changes of torsional frequency responses with exciting forces for central element of the drive system, it is known:

As the exciting forces grow, the amplitudes of frequency responses increase. However, the natural frequency of the system is unchanged. It is because the exciting forces do not change the natural characteristics. The effects of exciting force on each element are similar.

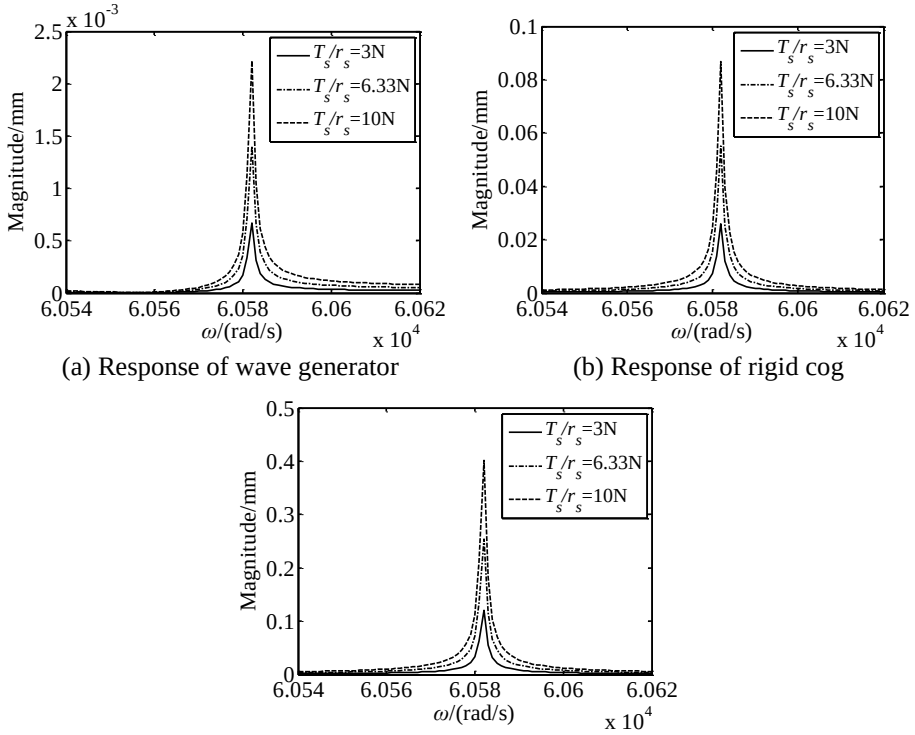

(a) Response of wave generator (b) Response of rigid cog

(c) Response of rotor

Fig. 6. Changes of torsional frequency responses with exciting forces

Fig. 7 gives changes of frequency responses with meshing stiffness of the rotor. It shows:

(1) As meshing stiffness of the rotor grows, the resonance frequency increases. The increment of frequency is larger when the meshing stiffness is smaller.

(2) The resonance amplitude of elements is smallest at $k_r = 1\times10^9$ N/m.

(3) The meshing stiffness affects the resonance frequency and amplitude at the same time. The reason is that the meshing forces increase with the changes of the meshing stiffness. And then the natural frequency increases with stiffness

proportionately. As the natural frequency increases, the modal shapes of movable tooth drive system change. These are the reasons for the change of resonance amplitude.

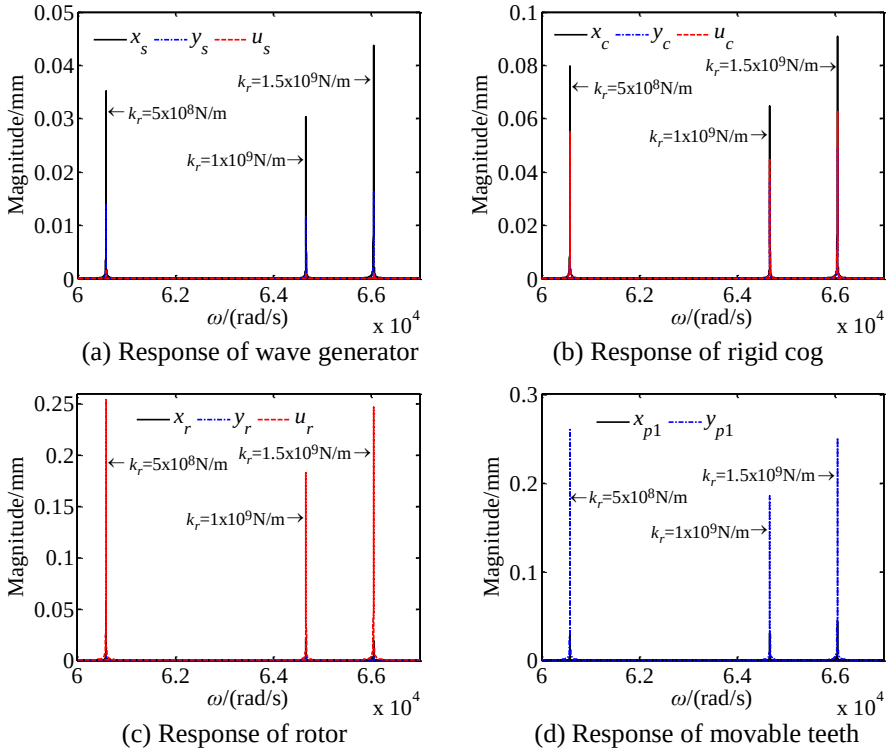

(a) Response of wave generator (b) Response of rigid cog

(c) Response of rotor (d) Response of movable teeth

Fig. 7. Changes of frequency responses with meshing stiffness of rotor

6. Conclusions

In this paper, a mesh-type rotary piezoelectric motor is proposed, and the working principle of the motor is illustrated. Besides, the dynamic models and equations of drive system for the proposed motor are established, and the force responses are investigated. Through theoretical research and numerical analysis, the laws of time responses and frequency responses were studied deeply. Results show:

(1) The displacements of torsional vibrations of central elements are larger than that of translational vibration when the system resonates.

(2) The largest amplitudes of elements occur in tangential direction.

(3) The displacement resonance of rotor is largest whether the parameters change or not.

The study of vibration characteristics of the motor can provide theoretical basis for parameters optimization of the mesh-type rotary piezoelectric motor.

Acknowledgment

This project is supported by National Natural Science Foundation of China (51605423) and Doctoral Scientific Research Foundation of Jiangsu University of Science and Technology (1022931704).

R E F E R E N C E S

[1]. *W. Wu, C. Pan and Y. Zhang,* "Piezotronics and piezophototronics - from single nanodevices to array of devices and then to integrated functional system", in Nano Today, vol. 8, no. 6, 2013, pp. 619-642.

[2]. *D. T. Qin,* "History and Process of science and technology on mechanical transmission", in Chin. J. Mech. Eng., vol. 39, no. 12, 2003, pp. 37-43.

[3]. *T. Morita,* "Miniature piezoelectric motors", in Sensors and Actuators, A: Physical, vol. 103, no. 3, 2003, pp. 291-300, Feb. 2003.

[4]. *J. P. Li, X. Q. Zhou, H. W. Zhao, M. K. Shao, N. Li, S. Z. Zhang and Y. M. Du,* "Development of a Novel Parasitic-Type Piezoelectric Actuator", in IEEE-ASME Transactions on Mechatronics, vol. 22, no. 1, 2017, pp. 541-550.

[5]. *C. Chen, Y. L. Shi, J. Zhang and J. S. Wang,* "Novel linear piezoelectric motor for precision position stage", in Chinese Journal of Mechanical Engineering (English Edition), vol. 29, no. 2, 2016, pp. 378-385.

[6]. *C. X. Hu, L. Cheng, Z. Wang, Y. B. Zheng, S. Bai and Y. Qin*, "A transparent antipeep piezoelectric nanogenerator to harvest tapping energy on screen", in Small, vol. 12, no. 10, 2016, pp. 1315-1321.

[7]. *A. K. Muhammad, S. Okamoto, and J. H. Lee*, "Computational simulations and experiments on vibration control of a flexible two-link manipulator using a piezoelectric actuator", in Engineering Letters, vol. 23, no. 3, 2015, pp.200-209.

[8]. *R. Q. Rudy, G. L. Smith and D. L. Devoe,* "Millimeter-scale traveling wave rotary ultrasonic motors", in Journal of Micro- electromechanical Systems, vol. 24, no. 1, 2015, pp.108-114.

[9]. *S. T. Ho and W. H. Chiu*, "A piezoelectric screw-driven motor operating in shear vibration modes", in Journal of Intelligent in Material Systems and Structures, vol. 27, no. 1, 2016, pp. 134-145.

[10]. *M. L. Renteria and V. Bolborici*, "A dynamic model of the piezoelectric traveling wave rotary ultrasonic motor stator with the finite volume method", in Ultrasonics, vol. 77, no. 1, 2017, 69.

[11]. *C. Chen, F. Li and X. J. Yan,* "Study on non-contact piezoelectric actuator with spherical rotors", in Proceedings of the CSEE, vol. 32, no. 6, 2012, pp. 163-169.

[12]. *Y. Hojjat and M. R. Karafi,* "Introduction of roller interface ultrasonic motor (RIUSM)", in Sensors and Actuators, A: Physical, vol. 163, no. 1, 2010, pp. 304-310.

[13]. *O. Barth*, "Harmonic piezodrive - miniaturized servo motor", in Mecha- tronics, vol. 10, no. 4, 2000, pp. 545-554.

[14]. *H. B. Xin and W. Z. Zheng*, "Study on harmonic piezomotor", in Piezoelectrics and Acoustooptics , vol. 26, no. 2, 2004, pp. 35-49.

[15]. *L. Z. Xu and X. J. Zhu*, "Natural frequencies and vibrating modes for a magnetic planetary gear drive", in Shock and Vibration, vol. 19, no. 6, 2012, pp. 1385-1401.